JOURNAL OF OPTOELECTRONICS AND ADVANCED MATERIALS Vol. 10, No. 11, November 2008, p. 3091 - 3100

Two-dimensional infrared correlation spectroscopic studies of polymer blends: conformational changes and specific interactions in polytetrahydrofuran / cholesteryl palmitate blends

M.-C. POPESCU*, C. VASILE
Romanian Academy, "Petru Poni" Institute of Macromolecular Chemistry, 41A Grigore Ghica Voda Alley, Iasi, Romania

Generalized two-dimensional infrared (2D IR) correlation spectroscopy has been applied to the study of the conformational changes and specific interactions in blends of polytetrahidrofuran (PTHF) and cholesteryl palmitate (CP). IR spectra have been measured for CP, PTHF, and their blends of different compositions: 2/98, 4/96, 6/94, 10/90, 16/84, 32/68, 64/36, and 80/20. In order to apply 2D IR correlation analysis the samples are divided into two sets for 2D: set A with high PTHF content 0/100, 2/98, 4/96, 6/94, 10/90, 16/84, 32/68 CP/ PTHF and set B with high CP content 64/36, 80/20 and 100/0 CP/PTHF. The 2D IR synchronous correlation analysis separates the bands of PTHF from those of CP. The 2D IR asynchronous correlation analysis produces cross-peaks that are indicative of the specific interaction or the conformational change in the blends. Ten "blend bands" are identified at 2916, 1441, 1243, 1227, 1106 and 967 cm^{-1} (CP) and 2802, 2862, 1492 and 1127 cm^{-1} (PTHF), whose origin has been attributed to the molecular level changes induced by mutual influence of the components which involve aliphatic CH and C-O-C groups of CP and PTHF, respectively.

(Received August 30, 2008; accepted October 30, 2008)

Keywords: Polymer blends, Liquid crystal, Blends, IR spectroscopy, 2D correlation spectroscopy

1. Introduction

Blending is regarded as an economical and efficient alternative for developing new polymeric materials, which allows the combination of desirable properties of different polymers with exceptional advantages over those of single or even novel polymeric materials.

Low molecular weight liquid crystals (LC's) in polymer matrices constitute interesting systems from many points of view. Many studies concerning phase behaviour, miscibility, morphology and properties have been done on such blends [1-13]. It has long been known that a LC can reduce the melt viscosity of polyolefin and polyester blends [14]. However, these effects are very similar to those induced by other small molecule additions especially lubricant of additives such as zinc stearate.

The incorporation of low molecular weight liquid crystals in amorphous polymers has been suggested as an alternative method to bring about modest improvements in the mechanical properties of polymeric composites [15-18]. Due to their mechanical anisotropy, which results from molecular alignment, the liquid crystal molecules may orient themselves in the shear field characteristic of a processing operation. Upon cooling, this orientation may impart to the composite some improvements in mechanical properties found with fibrous reinforcements, but with the advantage that the additive acts also as a plasticizer.

Polymer blends and composites can be used as self supported membranes for selective transport of gases and ions, optical valves, Bragg gratings films for holographic investigations, gas flow and pressure sensors, optical amplifiers, laser deflectors, memory and optoelectronic devices, textile industry and others. In the textile industry, these polymers are used to produce

fibers with high strength, which are used to make such items as helmets and bulletproof vests.

Polytetrahydrofuran (PTHF) and cholesteryl palmitate (CP) have a wide applicability especially in the textile industry. Cholesteryl palmitate has a structure similar to that of lanoline, which is in sheep's wool, hence the relationship with the textile industry, because of interests in obtain some finished articles from synthetic polymers with similar properties to naturals products.

PTHF is one of the main components in polyurethanes structure. Polyurethanes are known by the variety of qualities they impart to the finished textiles, such as: antibacterial protection, the winding modification of surface, antistatic effect, hydrophilicity, uniform painting, resistance at washing, a good fixing of the colors, and non-woven finishing**.**

The addition of some low molecular weight compounds to polymers yields improvements in the life time and processing of the polymers. By covering the textile materials with polymeric compounds one can obtain products with special properties and large applicability.

Generalized tow-dimensional (2D) IR correlation spectroscopy, proposed by Noda in 1986 [19], has

attracted considerable attention in the last decades for its wide applicability compared with conventional one-dimensional spectra. This novel 2D method can handle spectral fluctuations as an arbitrary function of time [20] or any other physical variables, such as temperature [21], pressure [22] or concentration [23, 24], among others. Following the pioneering work of Noda, many research groups have adopted 2D correlation analysis to study self-associated molecules [25], polymers [26], liquid crystals [27, 28] and biological molecules, such as peptides [29] and proteins [30].

Vibrational spectroscopic studies on polymer blends have been largely restricted to those containing hydrogen bonds and they have mainly involved infrared spectroscopy [31, 32]. Hydrogen bonds are often employed to enhance the miscibility in polymer blends [33] and infrared spectroscopy is powerful in investigating hydrogen bonds [33]. In contrast, vibrational spectroscopic studies on the specific interactions in polymer blends without hydrogen bonding have been less often reported [34]. The studied system in this paper adds new data in this field.

In the case of polymer blends, the technique of two-dimensional 2D IR correlation spectroscopy offers new possibilities for the analysis and interpretation of vibrational spectra. 2D correlation analysis is performed from a set of spectra collected from a system under an external perturbation that induces alterations in the spectrum of the system. In the 2D approach, the bands are spread over the second dimension, thereby simplifying the visualization of spectra consisting of overlapping bands. Inter- and intra-molecular interactions can be investigated by correlating absorption bands from different functional groups or parts of a molecule.

PTHF/CP blends with different composition were studied by thermogravimety (TG) and differential scanning calorimetry (DSC). Thermogravimetric data were used to establish the degree of interaction in blends [35, 36]. It has been established that PTHF/ CP blends are characterized by good thermal stability.

In the present study, FT-IR spectroscopy and generalized 2D IR correlation spectroscopy have been applied to explore the intermolecular interactions in blends of polytetrahydrofuran (PTHF) and cholesteryl palmitate (CP).

2. Experimental

2.1. Materials

As semi - crystalline isotropic polymeric compound, PTHF, was used. It is a commercial product purchased from BASF, having a $\overline{M}_n = 2000\,g/mol$, with the following chemical formulae:

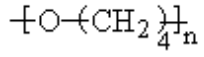

CP was used as a low-molecular-weight additive. It was purchased from Nopris SRL, Cluj Napoca, Romania, and used as received. It has the following structure:

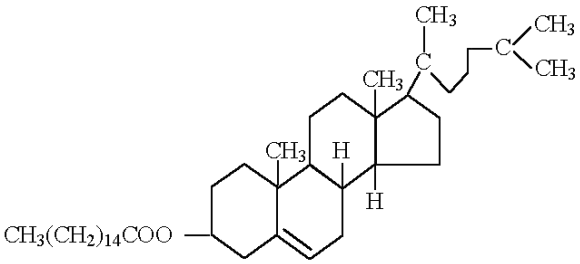

CP is a compound with liquid crystalline properties characterized by two types of mesophases: i.e. cholesteric (Ch) and smectic (S) mesophases. Monotropic phases are obtained from an isotropic melt (I) in agreement with DSC, (4° C/min) determinations. The transitions between these phases are: (C→Ch) at 74.5 °C; (Ch→I) at 80 °C; and (Ch→S) at 73.5 °C.

2.2. Blends preparation

Semi-crystalline PTHF and liquid crystalline CP were separately dissolved in 1, 2-dichloroethane (DCE) to form 0.8 g/dL solutions. The solutions were mixed to the following CP/PTHF ratios (wt/wt): (1) 2/98, (2) 4/96, (3) 6/94, (4) 10/90, (5) 16/84, (6) 32/68, (7) 64/36, and (8) 80/20. The mixtures of solutions were stirred for 5 h. After that, the solvent was slowly evaporated at room temperature. To remove the residual solvent and moisture, the samples were dried in a vacuum oven at 50°C for 2–6 days and total removal of the solvent was checked by IR spectroscopy.

2.3. Investigation methods

FT-IR Spectroscopy

FT-IR spectra were recorded on solid samples in KBr pellets by means of a FT-IR DIGILAB Scimitar Series spectrometer (USA) with a resolution of 4 cm^{-1}. The concentration of the samples in the tablets was constant at 5 mg/500 mg KBr. Five recordings were performed for each sample after successive milling and the evaluations were made on the average spectrum obtained from these five recordings. Processing of the spectra was done by means of Grams/32 program (Galactic Industry Corp.).

2D correlation spectroscopy

2D FT-IR correlation intensities were calculated using MATLAB program derived from the generalized 2D correlation method developed by Noda [19].

The FT-IR spectra of PTHF and its blends with CP were divided into two sets: set A and set B [37]. Set A contains the FT-IR spectra of 1) PTHF, 2) 92% PTHF - 8% CP, 3) 84 % PTHF-16% CP and 4) 68% PTHF-32% CP. Set B contains the FT-IR spectra of 5) 36% PTHF-64% CP, 6) 20% PTHF-80% CP and 7) CP. The spectra in

set A were arranged in the order 1-2-3-4. The spectra in set B were arranged in the order 5-6-7. Thus, in both sets, the intensities of the bands of PTHF are decreasing while those of CP are increasing. The reference spectra used for set A and B were those of 1 and 5, respectively.

In 2D correlation analysis, two kinds of correlation maps synchronous and asynchronous are generated from a set of dynamic spectra obtained from the modulation experiment [38]. According to reference [37], using the function Φ to designate synchronous 2D correlation, the intensities between two bands, can be written by the following relations:

$$\Phi[\nu(\text{PTHF}),\nu(\text{PTHF})] > 0 \qquad \Phi[\nu(\text{CP}),\nu(\text{CP})] > 0$$
$$\Phi[\nu(\text{PTHF}),\nu(\text{CP})] < 0 \qquad \Phi[\nu(\text{CP}),\nu(\text{PTHF})] < 0$$

Based on these relations, it is possible to ascribe bands in the spectra of the blends to PTHF or CP.

An asynchronous correlation peak appears only if the intensity change of two bands at ν_1 and ν_2 has basically dissimilar trends. According to Noda [37] $\Phi[\nu_1, \nu_2] < 0$ and $\Psi[\nu_1, \nu_2] > 0$ imply that the intensity change at ν_1 occurs at higher PTHF content compared to that at ν_2. So do $\Phi[\nu_1, \nu_2] > 0$ and $\Psi[\nu_1, \nu_2] < 0$. $\Phi[\nu_1, \nu_2] < 0$ and $\Psi[\nu_1, \nu_2] < 0$ imply that the intensity change at ν_1 takes place at lower PTHF content than that at ν_2. So do $\Phi[\nu_1, \nu_2] > 0$ and $\Psi[\nu_1, \nu_2] > 0$. When an asynchronous peak $\Psi[\nu_1, \nu_2]$ appears between two bands at ν_1 and ν_2, it can be either due to the conformational change of the component polymers in their blends or to the specific interactions between the component polymers [37]. If the sequential order between ν_1 and ν_2 in set A is reversed in set B, then the band at ν_1 and ν_2 can be regarded as indicative of the specific interactions between PTHF and CP.

3. Results and discussion

3.1. FT-IR spectra interpretation

The spectra of the blends obtained at room temperature contain all bands corresponding to the components (Fig. 1). A detailed examination of the spectra shows changes in the 2750–3000 cm^{-1} and 900–1700 cm^{-1} regions.

Spectral modifications occurred in blends of PTHF/CP and bands positions were better evidenced by the second derivative method. Generally, the second derivative IR spectra can obviously enhance the apparent resolution and amplify tiny differences of the IR spectrum. The second derivative of the IR spectra (Fig. 2) were obtained with the Savitsky-Golay method (second- order polynomial with fifteen data points) using Grams 32 program. The exact frequencies appearing in Table 1 and 2 come from the following second derivative method and 2D correlation analysis. The assignment of bands was made using reference [39].

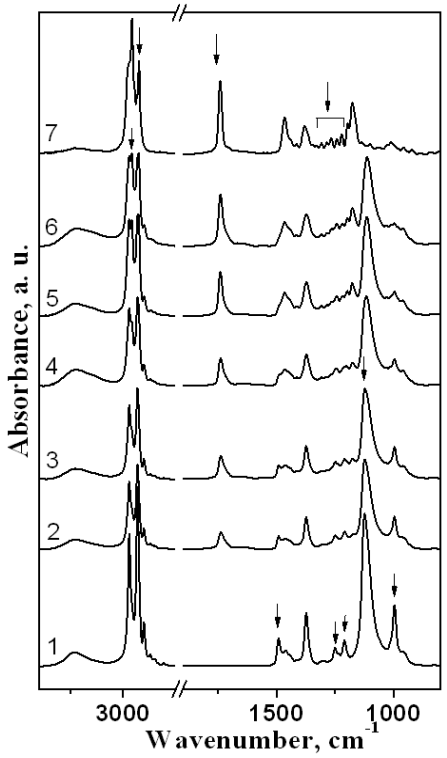

Fig. 1. FT-IR spectra of the pure components and blends recorded at room temperature in 500-4000 cm^{-1} region: (1) PTHF, (2) 8 CP/92 PTHF, (3)16 CP/84 PTHF, (4) 32 CP/68 PTHF, (5) 64 CP/36 PTHF, (6) 80 CP/20 PTHF, (7) CP.

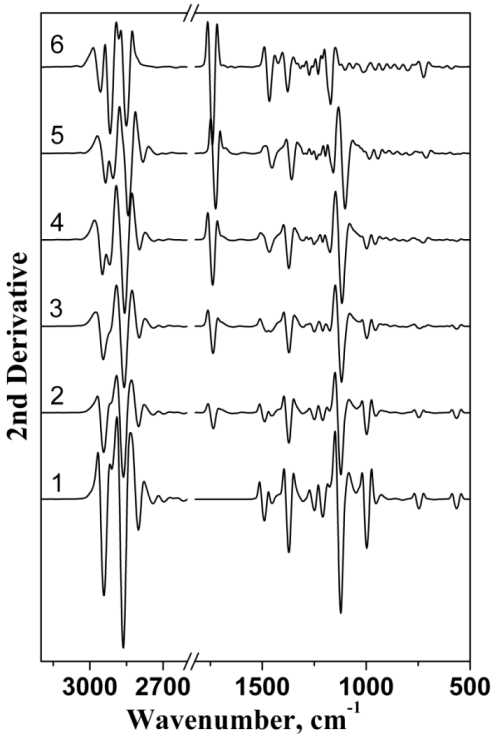

Fig. 2. Second derivatives of the FT-IR spectra of the pure components and blends: (1) PTHF, (2) 16 CP/84 PTHF, (3) 32 CP/68 PTHF, (4) 64 CP/36 PTHF, (5) 80 CP/20 PTHF, (6) CP.

Table 1. Bands assignments to PTHF in FTIR spectra.

ν (cm^{-1})	assignments
2942	CH_3 symmetric stretching
2864	CH_2 symmetric stretching
2842	CH_2 symmetric stretching
2826	CH stretching
2804	CH stretching
1491	CH_3 asymmetric bending
1475	CH_2 deformation
1460	CH_2 deformation
1372	CH_3 symmetric bending
1249	C-O asymmetric stretching
1231	C-O asymmetric stretching
1209	C-O stretching or C-C stretching
1127	C-O-C symmetric stretching
1104	C-O-C asymmetric stretching
1056	C-O-C asymmetric stretching
1019	C-O stretching
996	CH deformation
951	CH deformation

From Figs. 1 and 2 it can be observed that upon increasing CP content in the blends, an increase of the absorbance of the bands at 2917 and 2854 cm^{-1} corresponding to the stretching vibrations (ν) of CH aliphatic groups and a decrease of the intensity of the band at 1490 cm^{-1} corresponding to the deformation vibration (δ) of CH aliphatic groups take place. In addition, the increase of the absorbance of the bands at 1267 cm^{-1}, 1242 cm^{-1}, 1221 cm^{-1} and 1196 cm^{-1} corresponding to the stretching vibrations (ν) of C-O group of CP and the decrease of the intensity of the bands at 1251 cm^{-1}, 996 cm^{-1} corresponding to the symmetric stretching vibrations of C-O-C groups and those at 1209 cm^{-1} and 1126 cm^{-1} corresponding to the anti-symmetric stretching vibration of C-O-C groups of PTHF were evident.

The band centred at 1730 cm^{-1} corresponding to the stretching vibration of C=O group shows an increase in intensity with increasing content of CP in the blends.

With the aim of establish whether the blending determined spectral changes, the pure components spectra were taken into account and on the basis of the additivity law, the calculated spectra of the blends were obtained and compared with the experimental ones (Fig. 3). For an immiscible blend the additive spectrum is overlapped with the experimental one, while for a miscible or partially miscible blend, differences such as frequency shifts, band broadening, and changes in the intensity of some bands caused by intermolecular interactions between components could appear. The differences could be attributed to some conformational changes, too.

Table 2. Bands assignments to CP in FT-IR spectra.

ν (cm^{-1})	assignments
2961	CH asymmetric stretching
2947	CH_3 asymmetric stretching
2916	CH_2 asymmetric stretching
2890	CH stretching
2869	CH_3 symmetric stretching
2849	CH_2 symmetric stretching
2827	CH stretching
1739	C=O stretching
1465	CH_3 asymmetric bending or C=C stretching
1436	CH_2 or CH_3 asymmetric deformation
1415	O-H amide deformation
1382	CH_3 symmetric bending
1328	CH deformation
1308	C-O asymmetric stretching
1283	C-O asymmetric stretching
1266	C-O asymmetric stretching
1242	C-O asymmetric stretching
1220	C-O asymmetric stretching
1197	C-O symmetric stretching
1177	C-O symmetric stretching
1135	C-O-C stretching
1100	C-O-C asymmetric stretching
1067	C-O-C asymmetric stretching
1030	C-C deformation
1011	C-C deformation
996	CH bending
980	CH bending

Differences between the experimental and calculated spectra in the 2700 – 3100 cm^{-1} and 900-1800 cm^{-1} regions were observed. In the 2700 – 3100 cm^{-1} region, the blends with low content of CP, one can observe a pronounced decrease of the intensity of bands from experimental spectra with respect to the calculated ones, especially the absorbance of the 2941 cm^{-1} and 2863 cm^{-1} bands corresponding to the stretching vibrations of the CH aliphatic groups. In the case of blends with high content of CP, the differences between experimental spectra and calculated ones, are very small. A small difference can be observed in the case of the 80% CP/ 20 % PTHF blend, between the intensities of the 2917 cm^{-1} and 2854 cm^{-1} bands assigned to stretching vibrations of CH aliphatic groups.

In the blends with low CP content in the 900 – 1800 cm^{-1} region differences between experimental and calculated spectra consist of a small increase of the intensity of the 1126 cm^{-1} band in calculated spectra with respect to the experimental one. This band is assigned to the asymmetric vibration of C-O-C groups and also a decrease of the 1730 cm^{-1} band corresponding to the vibration of C=O groups is evidenced. At high content of CP, the intensities of these

bands are highest in experimental spectra compared with the calculated spectra. The 1490 cm^{-1} band, assigned to deformation vibrations of CH aliphatic groups, and the 996 cm^{-1} band, assigned to symmetric stretching vibrations of C-O-C groups, shows small decreases of the intensity in the experimental spectra with respect to the calculated one.

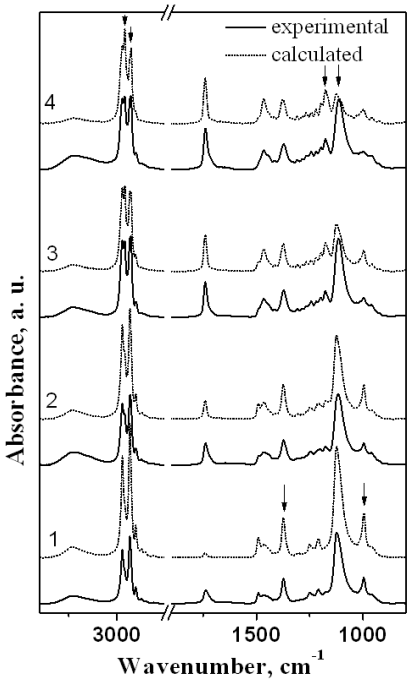

Fig. 3. Experimental (–) and calculated (••) FT-IR spectra in 500-4000 cm^{-1} region: (1) 8 CP/92 PTHF, (2) 32 CP/68 PTHF, (3) 64 CP/36 PTHF, (4) 80 CP/20 PTHF.

The specific interactions in polymer blends have been studied in line with the "interaction spectrum" [40]. The interaction spectrum of a blend is obtained by subtracting the spectra of both component polymers in the pure form (taking into account their weight proportion in blends) from the blend spectrum, thus representing only the net interaction between the component polymers.

From the analysis of the differences between experimental and calculated spectra in the 2700-3100 cm^{-1} region (Fig. 4) it can be observed, in the blends with CP content lower than 50 %, that the 2942 cm^{-1} and 1863 cm^{-1} bands, show a high intensity in the calculated spectra in respect with experimental ones, the differences being negatives. In the blends with CP content higher than 50 % the differences between calculated and experimental spectra are less pronounced. Thus, in the case of the blend with 64 wt% CP content are not evidenced significant differences, while in the case of the blend with 80 wt% CP content, in the experimental spectrum in respect with the calculated one, the intensities of 2917 cm^{-1} and 2863 cm^{-1} bands show a gentle decrease. In 900-1800 cm^{-1} region, it can observe the negative bands at 1491 cm^{-1}, 1373 cm^{-1} and 996 cm^{-1}, bands whose intensities decrease in the same time with increasing of CP content. The band at 1730 cm^{-1} is positive at low CP content and negative at high CP content. It can be also observed, the appearance of the 1725 cm^{-1} band, which indicates the fact that the band from 1730 cm^{-1} is broaded in the experimental spectrum in respect with calculated one. On low content of CP (less than 50 %) also, can be observed the appearance of a negative band at 1125 cm^{-1} which is obtained from difference between experimental and calculated spectra of the 1120 cm^{-1} band. The intensity of this band decreases in the same time with the increasing CP content. On high CP content (up than 50 %) this difference is positive and shifts to 1114 cm^{-1}.

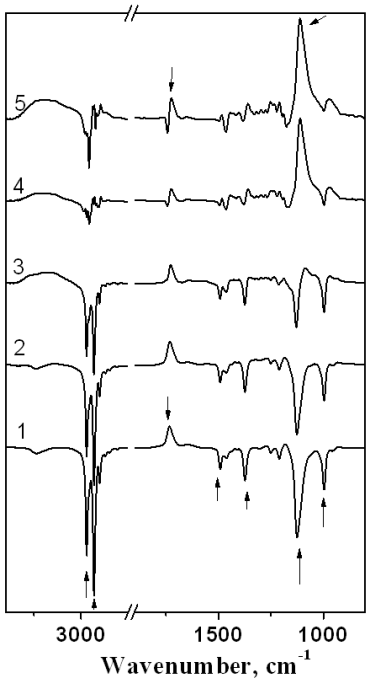

Fig. 4. Interaction (difference) spectra in 500-4000 cm^{-1} region: (1) 8 CP/92 PTHF, (2) 32 CP/68 PTHF, (3) 64 CP/36 PTHF, (4) 80 CP/20 PTHF.

The changes which appear can be assigned to some interactions between blend components, conformational changes of phase transitions.

3.2. 2D-IR correlation spectroscopy results

Generalized 2D correlation spectroscopy, which enhances similarities and differences in the variations of individual spectral intensities, is powerful in analyzing the rather complicated IR region, and may be able to identify spectral signatures of the specific interaction in polymer blends.

In the spectral region from 3100-2700 cm^{-1} of PTHF and CP the bands are due to aliphatic CH stretching vibrations. In Figures 5, 6 and 7 are presented synchronous and asynchronous correlation maps of calculated (Figure 5) and set A and B for experimental (Figs. 6, 7) data in this region.

The synchronous and asynchronous correlation maps for calculated data of set A and set B in this region are similar. In synchronous spectrum two auto-peaks at 2866

and 2917 cm^{-1}, three positive cross-peaks (un-shaded) at 2966 vs. 2917 cm^{-1}, 2943 vs. 2866 cm^{-1} and 2866 vs. 2800 cm^{-1} and four negative cross-peaks (shaded) at 2943 vs. 2917 cm^{-1}, 2966 vs. 2866 cm^{-1}, 2917 vs. 2866 cm^{-1} and 2917 vs. 2800 cm^{-1} were evidenced. The assignment of the bands to CP and PTHF is consistent with the sign of the cross-peaks. The cross-peak is positive for bands due to the same components of blend and negative for bands due to different components.

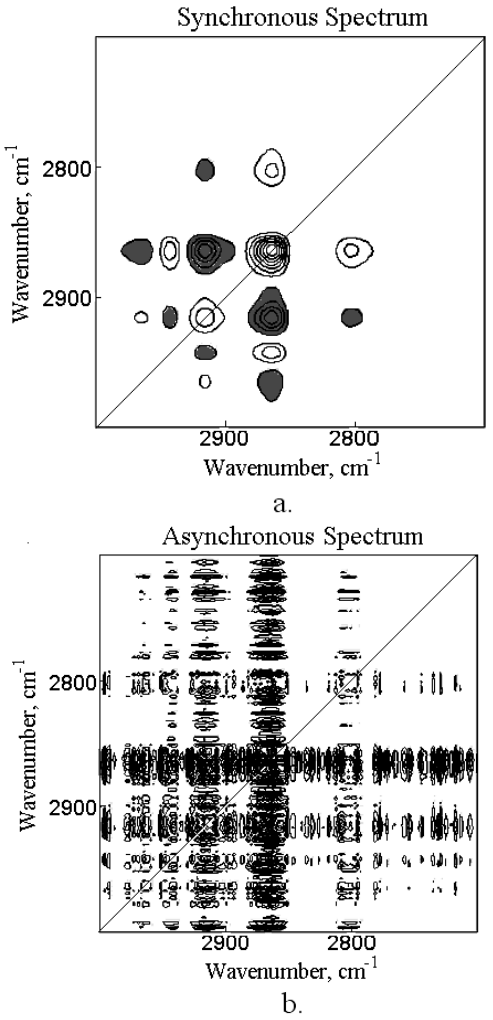

Fig. 5. Synchronous (a) and asynchronous (b) 2D FT-IR correlation spectra in the range of 3000-2700 cm^{-1}, drawn from the calculated FT-IR spectra of set A and set B.

The band at 2800 cm^{-1} belongs to PTHF. This band has positive correlation with the band at 2866 cm^{-1} and negative correlation with the band at 2917 cm^{-1}. This fact indicate that the band at 2866 cm^{-1} is also due to the PTHF, whilst the band at 2917 cm^{-1} is due to CP, and that the intensity change of the bands at 2866 and 2800 cm^{-1} has the same direction and opposite direction with band at 2917 cm^{-1}. In similar mode the band at 2966 assigned to the CP and the band at 2943 cm^{-1}can be assigned to the PTHF. The asynchronous spectrum from calculated data has a characteristic aspect [41,42].

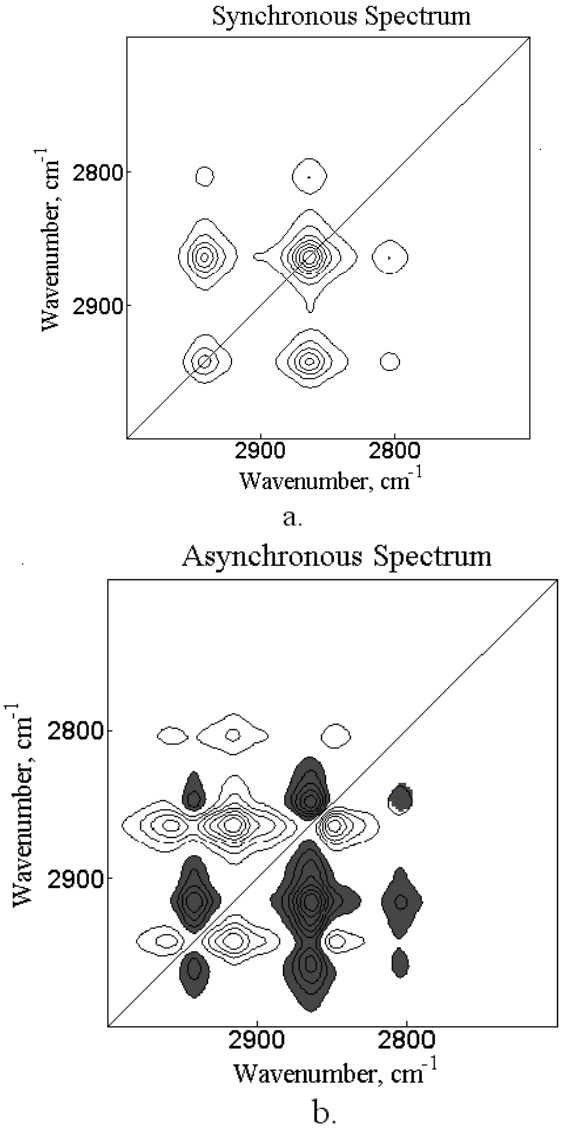

Fig. 6. Synchronous (a) and asynchronous (b) 2D FT-IR correlation spectra in the range of 3000-2700 cm^{-1}, drawn from the FT-IR spectra of set A.

As it has mentioned set A consists in PTHF and three its blends with CP having low CP content (92-64 wt% PTHF). The synchronous spectrum in 3000-2700 cm^{-1} region of this set is presented in Figure 6a. In this spectrum all peaks are positives and all bands are due to PTHF. The band at 2804 cm^{-1} should be due to PTHF, as can be seen from the second derivative in Figure 2. Therefore, the positive cross-peaks at 2943 vs. 2866 cm^{-1}, 2943 vs. 2804 cm^{-1} and 2866 vs. 2804 cm^{-1} indicate that the bands at 2943 cm^{-1} and 2866 cm^{-1} are all due to PTHF. Both PTHF and CP have strong bands in this region. However, only the coordinated intensity variation among PTHF bands is detected, while that among CP band does not appear. The coordinated intensity variation between CP bands and PTHF bands does not appear. Consequently, one may conclude that CP bands in this frequency range should be influenced significantly by the structural change, when mixed with PTHF.

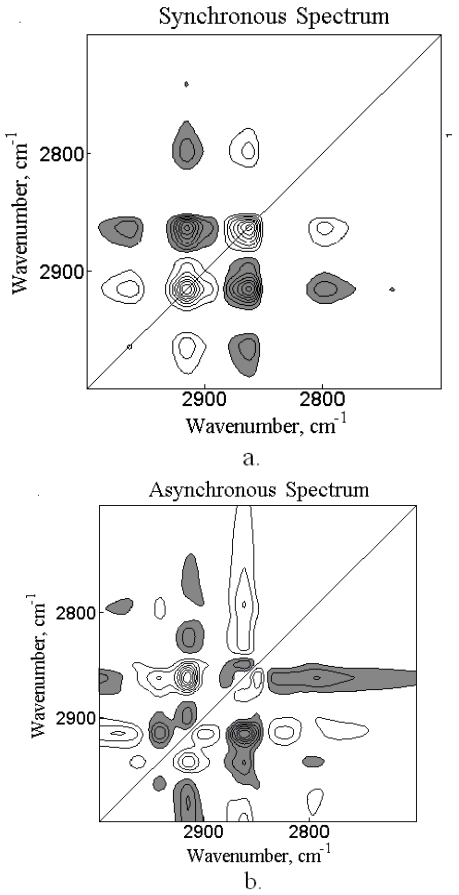

Fig. 7. Synchronous (a) and asynchronous (b) 2D FT-IR correlation spectra in the range of 3000 – 2700 cm^{-1}, drawn from the FT-IR spectra of set B.

The synchronous spectrum for set B (Fig. 7a) show both positive and negative cross-peaks. This spectrum is very different from that which corresponding to set A, being closer to the calculated one. So, two positive cross-peaks at 2964 vs. 2917 cm^{-1} and 2866 vs. 2800 cm^{-1} and four negative cross-peaks at 2964 vs. 2866 cm^{-1}, 2917 vs. 2866 cm^{-1}, 2917 vs. 2800 cm^{-1} and 2917 vs. 2740 cm^{-1} are seen in the left up side of the synchronous correlation spectrum. All positive cross-peaks in Fig. 7a related to the bands of the same compound, while the negative cross-peaks related to the bands of different components. As shown in Table 1, the band at 2800 cm^{-1} comes from PTHF. This band form positive cross-peak with the band at 2866 cm^{-1} and negative cross-peak with that at 2917 cm^{-1}; this means that the band at 2866 cm^{-1} corresponds to PTHF and that at 2917 cm^{-1} corresponds to CP. Similarly, the band at 2964 cm^{-1} is assigned to CP. The band at 2740 cm^{-1} appears only in synchronous spectrum of set B. According to its negative correlation with the CP band at 1917 cm^{-1}, it is assigned to PTHF.

The corresponding asynchronous spectra are shown in Fig. 6b and 7b. All peaks from Figures 6b and 7b imply out-of-phase variations between CP bands and PTHF bands. In Figure 6b of set A, four new bands are evidenced at 2848 cm^{-1}, 2916 cm^{-1}, 2927 cm^{-1} and 2959 cm^{-1}. The bands at 2848 cm^{-1} and 2916 cm^{-1} have out of phase variations with PTHF bands at 2804 cm^{-1} and 2866 cm^{-1}, and most probably they come from CP. The bands at 2927 cm^{-1} and 2959 cm^{-1} have in-phase variations with PTHF bands; in consequence, these bands correspond to PTHF and result by splitting of 2843 cm^{-1} band of PTHF.

It is seen, by comparing Figures 6b and 7b, that the asynchronous peaks at 2958 cm^{-1} vs. 2927 cm^{-1}, 2958 cm^{-1} vs. 2866 cm^{-1}, 2958 cm^{-1} vs. 2803 cm^{-1}, 2916 cm^{-1} vs. 2803 cm^{-1}, 2848 cm^{-1} vs. 2803 cm^{-1}, 2927 cm^{-1} vs. 2916 cm^{-1}, 2927 cm^{-1} vs. 2848 cm^{-1} appear only in set A, while those at 2964 cm^{-1} vs. 2942 cm^{-1}, 2980 cm^{-1} vs. 2916 cm^{-1}, 2942 cm^{-1} vs. 2863 cm^{-1}, 2942 cm^{-1} vs. 2795 cm^{-1}, 2863 cm^{-1} vs. 2795 cm^{-1}, 2863 cm^{-1} vs. 2826 cm^{-1}, 2942 cm^{-1} vs. 2916 cm^{-1}, 2916 cm^{-1} vs. 2900 cm^{-1}, 2916 cm^{-1} vs. 2826 cm^{-1}, 2980 cm^{-1} vs. 2795 cm^{-1}, 2916 cm^{-1} vs. 2777 cm^{-1}, 2880 cm^{-1} vs. 2863 cm^{-1} appear only in set B. All of these peaks should reflect the particular conformational features of set A and set B. The band at 2927 cm^{-1} is not identified in Fig. 7b, while the bands at 2980 cm^{-1}, 2942 cm^{-1}, 2900 cm^{-1}, 2880 cm^{-1}, 2826 cm^{-1} and 2777 cm^{-1} are not identified in Fig. 6b. In addition the bands at 2866 cm^{-1} and 2803 cm^{-1} from set A are shifted to 2863 cm^{-1} and 2795 cm^{-1} in set B.

The order of intensity variation between two bands is listed in Table 3 and Table 4 for set A and set B, respectively.

Table 3. Synchronous and asynchronous 2D correlation intensities and order of intensity variation between two bands of set A

No	Φ	Ψ	Assignment	Order*
1	Φ(2866, 2848)>0	Ψ(2866, 2848)<0	(PTHF, CP)	2866 after 2848
2	Φ(2916, 2866)>0	Ψ(2916, 2866)>0	(CP, PTHF)	2916 before 2866
3	Φ(2927, 2848)>0	Ψ(2927, 2848)<0	(PTHF, CP)	2927 after 2848
4	Φ(2848, 2803)>0	Ψ(2848, 2803)>0	(CP, PTHF)	2848 before 2803
5	Φ(2941, 2916)>0	Ψ(2941, 2916)<0	(CP, PTHF)	2916 after 2803
6	Φ(1492, 1106)>0	Ψ(1492, 1106)<0	(PTHF, CP)	1492 after 1106
7	Φ(1441, 1127)>0	Ψ(1441, 1127)>0	(CP, PTHF)	1441 before 1127
8	Φ(1388, 1127)<0	Ψ(1388, 1127)>0	(CP, PTHF)	1388 after 1127
9	Φ(1310, 1127)<0	Ψ(1310, 1127)>0	(CP, PTHF)	1310 after 1127
10	Φ(1288, 1127)<0	Ψ(1288, 1127)>0	(CP, PTHF)	1288 after 1127
11	Φ(1269, 1127)<0	Ψ(1269, 1127)>0	(CP, PTHF)	1369 after 1127
12	Φ(1243, 1127)>0	Ψ(1243, 1127)>0	(CP, PTHF)	1243 before 1127
13	Φ(1227, 1127)>0	Ψ(1227, 1127)>0	(CP, PTHF)	1227 before 1127
14	Φ(1127, 967)>0	Ψ(1127, 967)>0	(PTHF, CP)	1127 before 967

Table 4. Synchronous and asynchronous 2D correlation intensities and order of intensity variation between two bands of set B.

No	Φ	Ψ	Assignment	Order*
1	Φ(2866, 2848)>0	Ψ(2866, 2848)<0	(PTHF, CP)	2866 after 2848
2	Φ(2916, 2866)>0	Ψ(2916, 2866)>0	(CP, PTHF)	2916 before 2866
3	Φ(2927, 2848)>0	Ψ(2927, 2848)<0	(PTHF, CP)	2927 after 2848
4	Φ(2848, 2803)>0	Ψ(2848, 2803)>0	(CP, PTHF)	2848 before 2803
5	Φ(2941, 2916)>0	Ψ(2941, 2916)<0	(CP, PTHF)	2916 after 2803
6	Φ(1492, 1106)>0	Ψ(1492, 1106)<0	(PTHF, CP)	1492 after 1106
7	Φ(1441, 1127)>0	Ψ(1441, 1127)>0	(CP, PTHF)	1441 before 1127
8	Φ(1388, 1127)<0	Ψ(1388, 1127)>0	(CP, PTHF)	1388 after 1127
9	Φ(1310, 1127)<0	Ψ(1310, 1127)>0	(CP, PTHF)	1310 after 1127
10	Φ(1288, 1127)<0	Ψ(1288, 1127)>0	(CP, PTHF)	1288 after 1127
11	Φ(1269, 1127)<0	Ψ(1269, 1127)>0	(CP, PTHF)	1369 after 1127
12	Φ(1243, 1127)>0	Ψ(1243, 1127)>0	(CP, PTHF)	1243 before 1127
13	Φ(1227, 1127)>0	Ψ(1227, 1127)>0	(CP, PTHF)	1227 before 1127
14	Φ(1127, 967)>0	Ψ(1127, 967)>0	(PTHF, CP)	1127 before 967

*ν_1 after (before) ν_2 means the intensity change of the band at ν_1 occurs at higher (lower) CP contents than that at ν_2

The asynchronous peaks at 2916 cm^{-1} vs. 2866 cm^{-1} and 2941 cm^{-1} vs. 2916 cm^{-1} appear in both Figures 6b and 7b. They have opposite sign from set A to set B (see Table 3 and Table 4-row 2 and 5). Thus, these asynchronous peaks are symptomatic of the specific interaction in the blends. The band at 2916 cm^{-1} is due to CH_2 stretching vibrations of CP, while the bands at 2866 cm^{-1} and 2942 cm^{-1} are due to CH_2 and CH_3 stretching vibration of PTHF. It is concluded that the CH_2 of CP and the CH_2 and CH_3 groups of PTHF are involved in the mixing probably – CH_2- chain fragments in PTHF are entangled with CH_3-$(CH_2)_{14}$- chain fragment in CP assuming a partial miscibility.

Fig. 8 show the synchronous correlation spectrum for calculated data in 900-1600 cm^{-1} region. This region is characteristic to C-O and C-O-C symmetric and asymmetric stretching vibration and also symmetric and asymmetric deformation vibration of CH aliphatic groups.

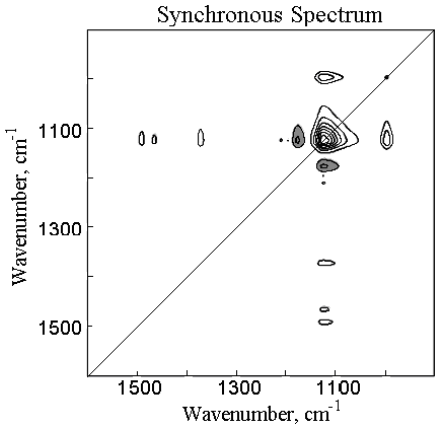

Fig. 8. Synchronous 2D FT-IR correlation spectra in the range of 1600-900 cm^{-1}, constructed from the calculated FT-IR spectra of set A and set B.

Two autopeaks at 1127 cm^{-1} and 996 cm^{-1}, four positive cross-peaks at 1492 vs. 1127 cm^{-1}, 1463 vs. 1127 cm^{-1}, 1382 vs. 1127 cm^{-1} and 1127 vs. 996 cm^{-1} and two negative cross-peaks at 1178 vs. 1127 cm^{-1} and 1211 vs. 1127 cm^{-1} were evidenced. The band at 1127 cm^{-1} is assigned to C-O-C symmetric stretching of PTHF. This band form positive cross-peaks with the bands at 1492 cm^{-1}, 1463 cm^{-1}, and 996 cm^{-1} that means that these bands correspond to vibrations of PTHF. The bands at 1178 cm^{-1} and 1211 cm^{-1} form negative cross-peak with the band at 1127 cm^{-1} that means that this band comes from CP.

In figures 9 and 10 are presented the synchronous and asynchronous correlation spectra for set A and B in this region. The synchronous correlation spectra for these sets are similar with those for calculated data in this region.

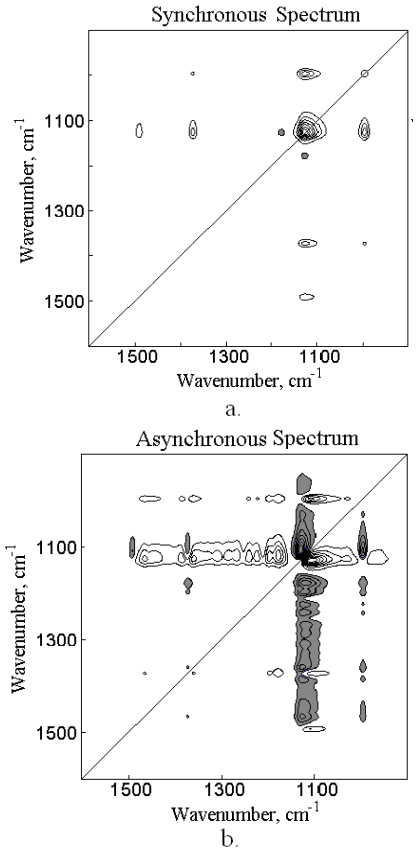

Fig. 9. Synchronous (a) and asynchronous (b) 2D FT-IR correlation spectra in the range of 1600 – 900 cm^{-1}, constructed from the FT-IR spectra of set A.

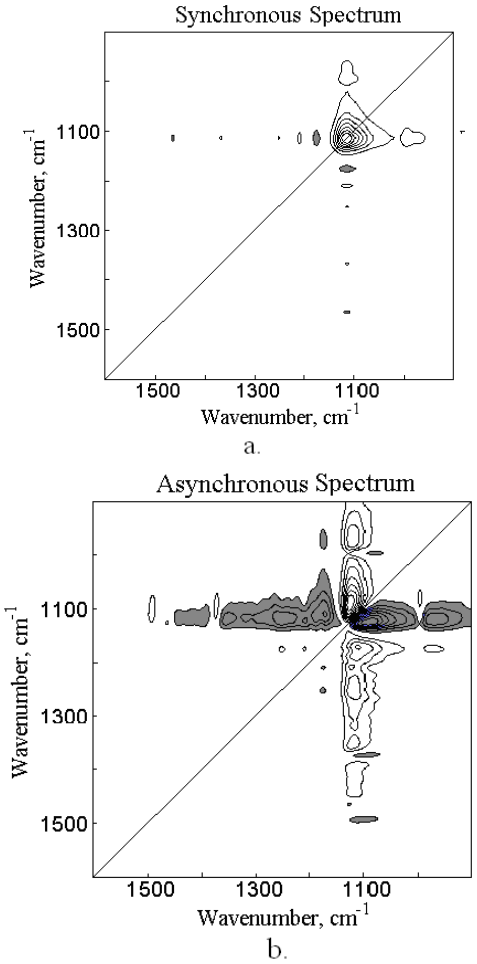

Fig. 10. Synchronous (a) and asynchronous (b) 2D FT-IR correlation spectra in the range of 1600 – 900 cm^{-1}, constructed from the FT-IR spectra of set B.

Some small differences were observed such as: in the calculated spectrum appear two peaks at 1492 cm^{-1} and 1463 cm^{-1} while in experimental spectra appear only one peak at 1492 cm^{-1} for set A and at 1465 cm^{-1} for set B. The peak at 1211 cm^{-1} is missing in the spectrum corresponding to set A, and the band from 1127 cm^{-1} is shifted to 1117 cm^{-1} in set B. Most probably, the changes that appear result from the specific interaction between blends components.

Asynchronous spectra are complex being made up of a great number of bands. Thus, in asynchronous spectra can be evidenced 19 bands from set A and 18 bands from set B. These bands form a great number of positive and negative cross peaks. In case of set A 12 bands have chose value with that from tables 1 and 2. Two new bands at 1361 and 1339 cm^{-1} were evidenced, and the band at 980 cm $^{-1}$ is shifted to 967 cm^{-1}. In case of set B only 5 bands have chose value with that from tables 1 and 2. Appear 3 new bands at 1081, 1353 and 1423 cm^{-1}, and the bands at 1382, 1308, 1197, 1100 and 1067 cm^{-1} are shifted to high wavenumber.

However, it is important to note that the signs of the asynchronous cross-peaks in Figure 9b are opposite to those in Figure 10b. It is seen by comparing Figures 9b and 10b that the asynchronous peaks at 1361 vs. 1127 and 1339 vs. 1127 appear only for set A, while those at 1423 vs. 1124, 1353 vs. 1124 and 1081 vs. 1124 cm^{-1} appear only for set B. All of these peaks should reflect the particular conformational features of set A and set B. The bands at 1361 and 1339 cm^{-1} are not identifiable in Figure 3. Since they have an asynchronous relationship with the PTHF band at 1127 cm^{-1}, they might be assigned to CP. Thus, the bands at 1361 and 1339 cm^{-1} are characteristic of the particular conformation of CP in set A. Judging from their frequencies, they are assigned to the OH or CH deformation vibrations. Similarly, the bands at 1423, 1353 and 1081 have an asynchronous relationship with the PTHF band at 1124 cm^{-1}, they might be assigned to CP, too. These bands can be assigned to OH or CH deformation and C-O-C asymmetric stretching vibrations and are characteristic of the particular conformation of CP in set B.

The asynchronous peaks at 1496 cm^{-1} vs. 1106 cm^{-1}, 1441 cm^{-1} vs. 1127 cm^{-1} , 1242 cm^{-1} vs. 1127 cm^{-1}, 1227 cm^{-1} vs. 1127 cm^{-1} and 1127 cm^{-1} vs. 967 cm^{-1} appear in both Figures 9b and 10b. They have opposite sign from set A to set B (see Table 3 and Table 4 - rows 6, 7, 12 -14). Thus, these asynchronous peaks are symptomatic of the specific interaction in the blends. The band at 1492 cm^{-1} and 1127 cm^{-1} is due to CH_3 bending and C-O-C stretching vibrations of PTHF, while the bands at 1441, 1243, 1227, 1106 cm^{-1} and 967 cm^{-1} are due to CH_2 deformation C-O stretching and CH bending vibration of CP. It is concluded that the CH_3 and C-O-C groups of PTHF and the CH_2, C-O and CH groups of CP are involved in the blend formation.

4. Conclusions

The present 2D FT-IR correlation spectroscopy study of composition-dependent spectral variations of PTHF – CP blends revealed in detail the composition-induced structural changes in the blends. 2D correlation analysis of the spectra of the seven samples divided into two sets enables us to elucidate the band assignment and the structural changes for each set.

The 2D synchronous correlation analysis separates the bands of PTHF from those of CP and detects bands that are not identified from the one-dimensional spectra of PTHF and CP. The 2D asynchronous correlation analysis reveals many out-of-phase band intensity variations that are indicative of the conformational change or the specific interaction in the blends.

The IR spectra are divided into two regions, and 2D correlation is performed on each region. The first region, from 3100-2700 cm^{-1}, is due to aliphatic CH stretching vibrations. The band at 2916 cm^{-1} due to the methyl groups of CP is a “blend band”. 2D correlation analysis of this region is useful both in identifying bands and cross-peaks representative of the specific interaction and in detecting coordinated band intensity variations common to set A and set B.

The second region, from 900-1600 cm^{-1}, is characteristic to C-O and C-O-C symmetric and asymmetric stretching vibration and also symmetric and asymmetric deformation vibration of CH aliphatic groups. In this region two asynchronous peaks which appear only for set A and three only for set B are evidenced. All of these peaks should reflect the particular conformational features of set A and set B and can be assigned to OH or CH deformation and C-O-C asymmetric stretching vibrations.

The bands at the bands at 1441, 1243, 1227, 1106 cm^{-1} and 967 cm^{-1} due to CP and 1492 cm^{-1} and 1127 cm^{-1} of PTHF are "blend bands". All of the asynchronous peaks in this region are indicative of the specific interactions in PTHF/CP blends. This region is most suitable for detecting the specific interactions in the polymer blends.

References

[1] M. Ballauff, Mol. Cryst. Liquid Cryst. **136**, 175 (1986).
[2] W. Ahn, C. Y. Kim, H. Kim, S. C. Kim, Macromolecule **25**, 5002 (1992).
[3] J. Y. Kim, C. H. Cho, P. Palffy-Muhoray, M. Mustafa, T. Kyu, Phys. Rev. Lett. **71**, 2232 (1993).
[4] H. Zhang, F. Li, Y. Yang, Sci. Chin. Ser B **38,** 412 (1995).
[5] C. Shen, T. Kyu, J. Chem. Phys. **102,** 556 (1995).
[6] H. W. Chiu, T. Kyu, J. Chem. Phys. **103,** 7471 (1995).
[7] T. Kyu, C. Shen, H. W. Chiu, Mol. Cryst. Liquid Cryst. **287** 27 (1996).
[8] H. W. Chiu, Z. L. Zhou, T. Kyu, Macromolecules **29**, 1051 (1996).
[9] J.R.S. Rodrigues, A. Kaito, V. Soldi, A.T.N. Pires, Polym. Int. **46,** 138 (1998).
[10] C. C. Riccardi, J. Borrajo, R. J. J. Williams, H. M. Siddigi, M. Dumon, J. P. Pascault, Macromolecules **31,** 1124 (1998).
[11] Z. Q. Lin, H. D. Zhang, Y. L. Yang, Macromol. Theor. Simul. **6,** 1153 (1997).
[12] M. Pracella, B. Bresci, Mol. Cryst. Liq. Cryst. Sci. Technol.,Sect. A **266,** 23 (1995).
[13] G. M. Russell, B. J. A. Paterson, C. T. Imrie, S. K. Heeks, Chem. Mater. **7,** 2185 (1995).
[14] A. Buckley, A. B. Conciatori, G. W. Calundann, US Patent 4, 434 262, 1984.
[15] K. F. Wissbrum, J. Rheol. **25,** 619 (1986).
[16] W. Huh, R. A. Weiss, L. Nicolais, Polym. Eng. Sci. **23,** 779 (1983).
[17] A. K. Kalkar, A. A. Bhalwankar, Polym. Sci. **2,** 573 (1994).
[18] A. K. Kalkar, V. V. Kunte, A. A. Deshpande, Macromol. New Front. Proc. IUPAC Int Symp Adv Polym Sci Technol, 1998.
[19] I. Noda, Appl.Spectrosc. **57**, 1049 (2003).
[20] T. Nakano, S. Shimada, R. Saitoh, I. Noda, Appl. Spectrosc **47,** 1337 (1993)**.**
[21] I. Noda, Y. Liu, Y. Ozaki, J. Phys. Chem. **100**, 8665 (1996).
[22] L. Smeller, K. Heremans, Vib. Spectrosc. **19**, 375 (1999).
[23] Y. Ren, M. Shimoyama, T. Ninomiya, K. Matsukawa, H. Inoue, I. Noda, Y. Ozaki, Appl. Spectrosc. **53**, 919 (1999).
[24] M. C. Popescu, M. Zanoaga, Y. Mamunya, V. Myshak, C. Vasile, J. Optoelectr. Adv. Mater. **4,** 923 (2007).
[25] Y. Ozaki, Y. Liu, I. Noda, Appl. Spectrosc. **51,** 526 (1997).
[26] T. Nakano, S. Shimada, R. Saitoh, I. Noda, Appl. Spectrosc. **47**, 1337 (1993).
[27] V. G. Gregoriou, S. E. Rodman, B. R. Nair, P. T. Hammond, J. Phys. Chem. B **106**, 11108 (2002).
[28] M. C. Popescu, D. Filip, C. Vasile, C. Cruz, J. M. Rueff, M. Marcos, J.L. Serrano, Gh. Singurel, J. Phys. Chem. B **110**, 14198 (2006).
[29] M. Muller, R. Buchet, U.P. Fringeli, J. Phys. Chem. **100**, 10810 (1996).
[30] Y. Wang, K. Murayama, Y. Myojo, R. Tsenkova, N. Hayashi, Y. Ozaki, J. Phys. Chem. **102,** 6655 (1998).
[31] W. H. Jo, C. A. Cruz, D. R. Paul, J. Polym. Sci., Part B:Polym. Phys. **27,** 1057 (1989).
[32] J. L. Koenig, M. J. M. Tovar, Appl. Spectrosc. **35**, 543 (1981).
[33] M. M. Coleman, J. F. Graf, P. C. Painter, Specific Interactions and the Miscibility of Polymer Blends, Technomic Publishing, Lancaster, PA, 1991.
[34] S. T. Wellinghoff, J. L. Koenig, E. Baer, J. Polym. Sci., Polym. Phys. **15**, 1913 (1977).
[35] D. Filip, C.I. Simionescu, D. Macocinschi, I. Paraschiv, J. Therm. Anal. **65**, 821 (2001).
[36] D. Filip, C.I. Simionescu, D. Macocinschi, Thermochimica Acta **395**, 217 (2002).
[37] Y. Ren, T. Murakami, T. Nishioka, K. Nakashima, I. Noda, Y. Ozaki, J. Phys. Chem. B **104,** 679 (2000).
[38] I. Noda, Appl. Spectrosc. **47,** 1329 (1993).
[39] D. W. Mayo, F. A. Miller, R. W. Hannah, Course notes on the interpretation of infrared and raman spectra, John Wiley & Sons, Inc. 2003.
[40] K. Nakasshima, Y. Ren, T. Nishioka, N. Tsubahara, I. Noda, Y. Ozaki, J. Phys. Chem. B **103,** 6704 (1999).
[41] C. Aghiorghiesei, M. C. Popescu, Gh. Singurel, l'Ecole d'Eté "Physico-chimie de l'atmosphère: des expériences de laboratoire aux campagnes de terrain", Iasi, Romania, 2006.
[42] M. C. Popescu, C. Vasile, Gh. Singurel, Polymers and Composites: Synthesis, Properties and Application, Eds: R.A. Pethrick, G. E. Zaikov et al., Chap 7, Nova Science Publishers, Inc. 71 (2007).

*Corresponding author: cpopescu@icmpp.ro